Energy Proceedings
Vol 26, 2022
ISSN 2004-2965

A heat-driven thermoacoustic heat pump with a single direct-coupling configuration capable of utilizing medium/low-grade heat for domestic applications#

Yiwei Hu[a,b], Jingyuan Xu[c*], Kaiqi Luo[d], Geng Chen[e], Limin Zhang[a], Zhanghua Wu[a], Ercang Luo[a,b*]

a. Chinese Academy of Science, Key Laboratory of Cryogenics, Technical Institute of Physics and Chemistry, Beijing 100190, China
b. University of Chinese Academy Science, Beijing 100049, China
c. Mechanical and Electrical Engineering Division, Karlsruhe Institute of Technology, Karlsruhe 76344, Germany
d. Building Energy Research Center, Tsinghua University, Beijing 100084, China
e. National Engineering Research Center of Power Generation and Safety, School of Energy and Environment, Southeast University, Nanjing 210096, China

ABSTRACT

This paper proposed a heat-driven thermoacoustic heat pump system capable of utilizing medium/low-grade heat for heating supply in domestic applications. The system consists of one simple thermoacoustic energy-conversion unit with a direct-coupling configuration, which greatly reduces the system complexity compared to the traditional multi-stage thermoacoustic systems. The dimensional parameters of the system were optimized under nominal conditions, with heat-sink and heat-source temperatures of 55 °C and 7 °C. Simulation results show that the proposed system can obtain a heating capacity of 5.7 kW and an overall coefficient of performance of 1.40 at nominal conditions. Economic performance shows annual fuel energy savings and energy cost savings for individual systems are 20.3 MWh/year and 675 $/year. The environmental assessments show that the proposed system can displace CO_2 emissions amounting to 3.72 tCO_2/year. Exergy loss of each component was then given better to understand the energy conversion processes of the system. Moreover, system performance under different heat-source and heat-sink temperatures was studied.

Keywords: Thermoacoustic heat pump; Building energy; Low/medium-grade heat recovery; Domestic heating; Energy saving; Energy conversion technology.

NONMENCLATURE

Symbols	
AE_{fric}	flow friction losses, W
AE_{Qw}	non-ideal heat transfer losses between the gas and the solid, W
AE_{Qx}	axial heat flow losses, W
C_s	energy cost savings, $
COP	coefficient of performance
c_{ng}	price of natural gas, $/kWh
f	frequency, Hz
f_{ng}	CO_2 emission factor of natural gas, $kgCO_2$/kWh
F	viscous pressure gradient
P	pressure amplitude, kPa
P_m	mean pressure, MPa
Pr	pressure ratio at the inlet of engine stage
Q_{demand}	demand heat supply, kW
$Q_{e,in}$	input heating power of the engine stage, kW
$Q_{e,out}$	output heating capacity of the engine stage, kW
$Q_{hp,in}$	input heating power of the heat pump stage, kW
$Q_{hp,out}$	output heating capacity of the heat pump stage, kW
Q_{out}	output heating capacity of the system, kW
q	instantaneous axial heat flux, W/m^2
q_F	heating load index, W/m^2
q_{ng}	calorific value of piped natural gas, MJ/m^3
q_w	heat flux between gas and solid
q_x	heat flux between gas and gas or between solid and solid
S_{mean}	per capita housing area, m^2/person
s_{family}	household size, person/household
T	temperature, K

* Corresponding author. Tel/Fax: +44 7422 527596 E-mail: jingyuan.xu@kit.edu (JY Xu)
Tel/Fax: +86 010 82543750 E-mail: ecluo@mail.ipc.ac.cn (EC Luo)

T_h	heating temperature, K
T_{source}	heat-source temperature, K
T_{sink}	heat-sink temperature, K
Greek letters	
η	relative Carnot efficiency, %
η_{boi}	efficiency of boiler, %
τ_{anu}	annual operating time, hour
uA	volumetric flow rate
Special symbol	
$\vert\ \vert$	magnitude of the complex number
∇	gradient of the complex number
Abbreviations	
CT	cavity structure
ER	emission reduction
FES	fuel energy savings
HHX	high-temperature heat exchanger
HSHX	heat-source heat exchanger
REG	regenerator
RT	resonant tubes
SHX	heat-sink heat exchanger
TBT	thermal buffer tube

1. INTRODUCTION

Thermoacoustic technology, as an emerging energy conversion technology, can be used for heating [1], cooling [2], or power generation [3]. This technology is not only environmentally friendly due to the use of pollution-free working gas, but also has a simple structure and contains no mechanical moving parts for a long fatigue life [4]. Current research on thermoacoustic heat pumps focuses on Stirling-type thermoacoustic heat pumps. In 2020, Cheng et al. proposed a beta-type Stirling heat pump driven by a linear motor which achieved a coefficient of performance (COP) of 1.8 [5]. In 2021, a linear-compressor-driven free-piston Stirling heat pump presented by Wang et al. achieved a COP of 2.41 [6]. Few studies have been reported on heat-driven thermoacoustic heat pumps. In 2020, Sun et al. proposed a free-piston Stirling heat pump driven by a Stirling engine, achieving a heating capacity of 6 kW and a COP of 1.8 [7]. While numerous research has reported high performance, the thermoacoustic heat pump is still in the early stages of development and the demonstrators reported are not viable for domestic applications due to the system complexity and the necessary use of high-temperature heat sources (>900 K). In this paper, we propose a first thermoacoustic heat pump capable of utilizing low/medium-grade waste heat, in particular aiming at domestic heating. The thermoacoustic heat pump consists of one simple thermoacoustic energy-conversion unit and has no moving parts. First, a numerical study including system performance and energy loss analysis was conducted to explore the operating characteristics. Then, the heat pump performance under different heat sink/source temperatures was investigated to assess the utility of the system. Finally, some conclusions are presented.

2. SYSTEM DESCRIPTION

2.1 Configuration

Fig. 1 presents the schematic of a heat-driven thermoacoustic heat pump. The system includes an engine unit, a heat pump unit, and a gas resonator unit in a loop. The engine unit consists of a heat-sink heat exchanger (SHX_e), a regenerator (REG_e), a high-temperature heat exchanger (HHX_e), and a thermal buffer tube (TBT_e). The cooler unit consists of a heat-sink heat exchanger (SHX_h), a regenerator (REG_h), a heat-source heat exchanger ($HSHX_h$), and a thermal buffer tube (TBT_h). *e* is for the engine stage and *h* is for the heat pump stage. The system works as follows: self-excited thermoacoustic oscillation begins and the conversion from heat to acoustic power occurs when the axial temperature gradient generated in the regenerator of the engine exceeds a critical value. The amplified acoustic power is used to drive the heat pump unit to pump heat from the heat source to the heat sink. Table 1 shows the geometric dimensions of the main components of the system.

2.2 Simulation model description

In this study, the numerical simulation of the heat-driven thermoacoustic heat pump is based on the SAGE program, which is widely used in modeling thermoacoustic devices [8-10].

Some important evaluating indicators are of interest. The coefficient of performance (COP) of the system can be expressed as

$$COP = \frac{Q_{out}}{Q_{e,in}} = \frac{Q_{e,out}+Q_{hp,out}}{Q_{e,in}} \tag{1}$$

where $Q_{e,out}$ and $Q_{hp,out}$ are the output heat from the SHX_e and SHX_h, respectively. $Q_{e,in}$ is the input heat to HHX_e.

Eq. (2) gives the relative Carnot efficiency of performance of the system,

$$\eta = \frac{COP}{\frac{T_{sink}}{T_h}+\frac{T_h-T_{sink}}{T_h}\times\frac{T_{sink}}{T_{sink}-T_{source}}} \tag{2}$$

where T_{sink} and T_{source} are the temperatures of the heat sink and heat source, respectively.

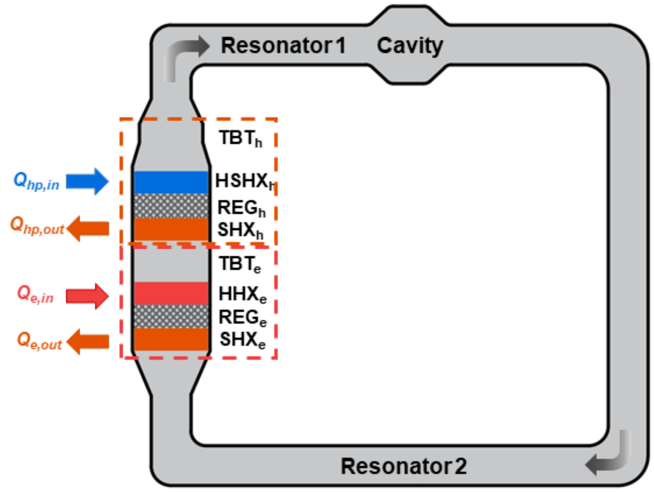

Fig.1. Schematic of a heat-driven thermoacoustic heat pump

Table 1
Dimensions of the components in each subunit.

Subunit	Parts	Diameter (mm)	Length (mm)	Other dimensions
Engine	SHX_e	150	33	Shell tube type, 11% in porosity, 1 mm in internal diameter
	REG_e	150	40	76% in porosity, 50 µm in wire diameter
	HHX_e	150	33	Shell tube type, 11% in porosity, 1 mm in internal diameter
	TBT_e	150	100	7 mm in wall thickness
Heat-pump	SHX_h	150	33	Shell tube type, 11% in porosity, 1 mm in internal diameter
	REG_h	150	35	71% in porosity, 50 µm in wire diameter
	$HSHX_h$	150	33	Shell tube type, 11% in porosity, 1 mm in internal diameter
	TBT_h	90	50	7 mm in wall thickness
	RT_1	54	2150	1E-3 in relative roughness
Gas resonator	CT	115	500	1 mm in wall thickness
	RT_2	54	9650	1E-3 in relative roughness

In addition to heating capacity and system efficiency, the fuel energy saving (*FES*), annual energy cost saving (C_s), and potential CO_2 emission reduction (*ER*) of this system have been explored to show the environmental and economic potentials of the system. *FES* is expressed as follows:

$$FES = \frac{Q_{out}}{\eta_{boi}} \times \tau_{anu} \quad (3)$$

where η_{boi} and τ_{anu} are the efficiency of the conventional boiler and annual operating time, respectively. η_{boi} is taken here to be 82% [11]. τ_{anu} can be simply calculated as $\tau_{anu} = Day_h \times 24\ h$. The annual heating days, Day_h, taking Beijing as an example, are generally 120 days [12].

$$C_s = \frac{Q_{out}}{\eta_{boi} \times q_{ng}} \times c_{ng} \times \tau_{anu} \quad (4)$$

where c_{ng} is the price of piped natural gas in China, which is 1.047 $\$/m^3$ according to the latest data [13]. q_{ng}, the calorific value of piped natural gas, is required to be greater than 31.4 MJ/m^3 in the relevant Chinese norms [14].

$$ER = \frac{Q_{out}}{\eta_{boi}} \times f_{ng} \times \tau_{anu} \quad (5)$$

where f_{ng} is the CO_2 emission factor of natural gas, 0.1836 $kgCO_2$/kWh [15].

3. SIMULATION RESULTS

3.1 Performance in nominal condition of the system

Table 2 gives the simulation results from SAGE in the nominal conditions of the system. The nominal conditions are based on the domestic heating applications: heat sink temperature is set at 55 °C, which is reported as the minimum temperature to prevent the harmful bacteria in the hot water supply [16]; heat source temperature is set at 7 °C according to the industrial standard in heat pump field [17]; the heating temperature in engine stage is chosen as 300 °C due to the intention of utilizing medium/low-grade temperature heat. The nominal heating capacity of 5.7 kW_{th} is chosen according to the typical domestic heating supply in China: taking ordinary low-rise residential buildings with energy-saving measures in Chinese towns as examples, the demand heat supply, Q_{demand} is calculated as follows:

$$Q_{demand} = S_{mean} \times s_{family} \times q_F \tag{6}$$

where S_{mean}, s_{family}, and q_F are the per capita housing area in Chinese towns, the household size, and the heating load index, respectively. Their values are 39.8 m^2/person [18], 2.62 person/household [19], and 55 W/m^2 [20] from relevant reports and specifications. A nominal heating capacity of 5.7 kW_{th} is thus obtained from Eq. 6. A coefficient of performance (COP) of 1.40 and a relative Carnot coefficient of performance (η) of 39.9% are obtained as well. Additionally, the cost savings and emissions assessments indicate that, this system has the potential to save 20.3 MWh of fuel energy consumption, 675 $ for an ordinary family, and to displace around 3.72 tons of CO_2 emission per year.

Table 2

Simulation results in nominal condition of the system

Symbol	Parameter	Value
P_m	Mean pressure (MPa)	10
Pr	Pressure ratio at the inlet of engine stage	1.07
T_h	Heating temperature of the engine stage (K)	573
T_{source}	Temperature of the heat source (K)	280
T_{sink}	Temperature of the heat sink (K)	328
f	Working frequency (Hz)	72.2
$Q_{e,in}$	Input heating power in engine stage (kW)	4.10
Q_{out}	Output heating capacity of the system (kW)	5.70
COP	Coefficient of performance of the system	1.40
η	Relative Carnot efficiency of the system	39.9%
FES	Annual fuel energy saving (MWh/year)	20.3
C_s	Annual energy cost saving ($/year)	675
ER	Annual potential CO_2 emission reduction (tCO_2/year)	3.72

3.2 Exergy losses analysis of the system

Exergy losses analysis allows for an accurate assessment of the system performance and provides guidance for subsequent improvement. The usual losses include flow friction losses (AE_{fric}), non-ideal heat transfer losses (AE_{Qw}) between the gas and the solid, and axial heat flow losses (AE_{Qx}). They are respectively calculated as

$$AE_{fric} = -T_0 \times \oint_{dt} \int_{dx} \frac{uAF}{T} \tag{6}$$

$$AE_{Qw} = -T_0 \times \oint_{dt} \int_{dv} \frac{q_w \cdot \nabla T_w}{T^2} \tag{7}$$

$$AE_{Qx} = -T_0 \times \oint_{dt} \int_{dv} \frac{q_x \cdot \nabla T_x}{T^2} \tag{8}$$

where uA and F are the volumetric flow rate and the viscous pressure gradient, q_w and ∇T_w are the heat flux and the temperature gradient between gas and solid, q_x and ∇T_x are the heat flux and the temperature gradient between gas and gas or between solid and solid.

Fig. 2 presents the exergy losses of the different components of this heat pump. The acoustic impedance is large in the regenerator, so the non-ideal heat transfer losses and axial heat flow losses account for most of the exergy losses. And in the resonant tubes, most losses come from the flow friction losses because of the large tube length. The optimization of these components can improve the system performance.

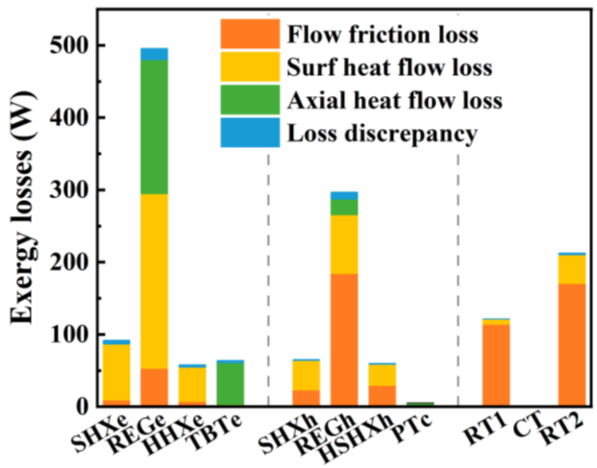

Fig. 2. Exergy losses analysis of the system in different components.

3.3 Effect of the heat-sink and heat-source temperatures

The operating conditions of domestic heat pumps are determined by environmental factors including heat-sink and heat-source temperatures, which significantly affect the heating performance of thermoacoustic heat pumps. Fig. 3 (a-d) show the effect of the heat-sink temperature on the heating performance under different heat-source temperature. The heat-source temperature varies between 260 K and 310 K, reflecting the variations in system performance over the seasons. The heat-sink temperature varies between 298 K and 363 K, covering the range of applications from low-temperature underfloor space heating to the provision of domestic hot water.

Generally, the input heating power, output heating capacity, and COP increase as the temperature difference between the heat-sink and heat-source decreases, while the η is on the contrary. Exceptionally, the variation of η at the heat-source temperature of 260 K, 270 K, and 280 K proves the existence of an optimal heat-sink temperature for the relative Carnot efficiency of the system. The thermoacoustic heat pump provides stable COP values over the temperature range considered, varying between 1.1 and 1.5 over most of the temperature range, which verifies that the proposed heat pump system supplies heat stably in a wide temperature range. Especially in the typical domestic heating supply temperature range of 50-70 °C, the proposed heat pump system can pump several kilowatts (1-11 kW) of heat from a heat source of 260 K to 310 K with remarkable efficiency.

4. CONCLUSION

A heat-driven thermoacoustic heat pump utilizing medium/low-grade heat for domestic heating applications has been studied in this paper. Numerical results prove the possibilities of practical applications with the heating capacity of 5.7 kW and the overall coefficient of performance (COP) of 1.40. Meanwhile, economic and environmental friendliness are demonstrated with the potential to save 20.3 MWh of fuel energy consumption, 675$ for an ordinary family, and to displace around 3.72 tons of CO_2 emission per year. Exergy losses analysis was further studied better to understand the energy conversion processes of the system. Moreover, influences of the heat-source and heat-sink temperatures were investigated to evaluate the system's adaptability to the varying operating conditions. In the future, a corresponding testbed will be established, and experimental work will be conducted to verify the simulation results.

ACKNOWLEDGEMENT

This work is supported by the National Natural Science Foundation of China (No. 51976230 and 51876213) and Leading Project A of Chinese Academy of Sciences (No. XDA21080300).

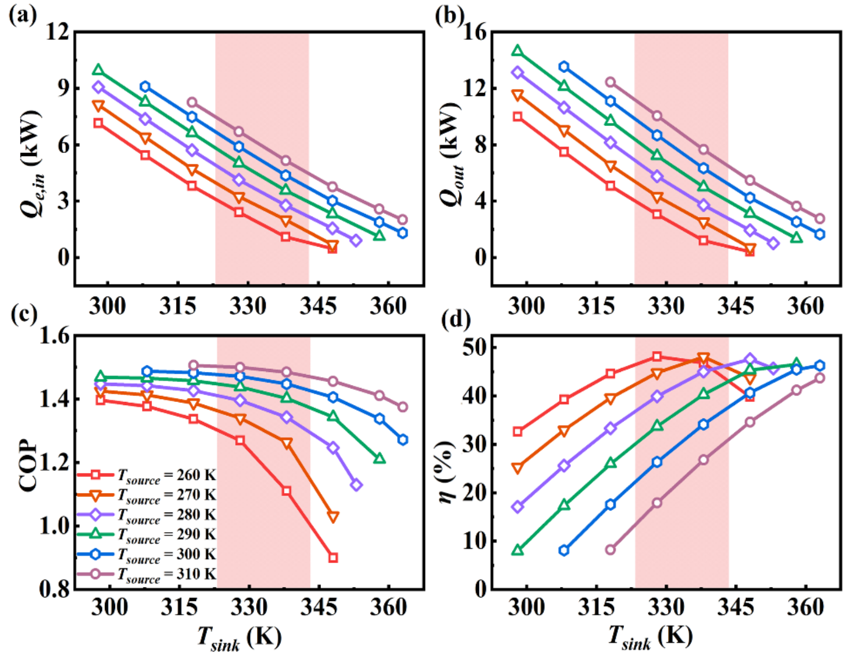

Fig. 3. Effect of the heat-sink and heat-source temperature on system performance. The highlighted area in pink relates to the typical domestic heating supply temperature range of 50-70 °C.

REFERENCE

[1] Widyaparaga A, Koshimizu T, Noda E, et al. The frequency dependent regenerator cold section and hot section positional reversal in a coaxial type thermoacoustic Stirling heat pump[J]. Cryogenics, 2011, 51(10): 591-597.

[2] Xu J Y, Yu G Y, Zhang L M, et al. Theoretical analysis of two coupling modes of a 300-Hz three-stage thermoacoustically driven cryocooler system at liquid nitrogen temperature range[J]. Applied Energy, 2017, 185(pt.2): 2134-2141.

[3] Xu J Y, Zhang L M, Hu J Y, et al. An efficient looped multiple-stage thermoacoustically-driven cryocooler for liquefaction and recondensation of natural gas[J]. Energy, 2016, 101: 427-433.

[4] Chen G, Tang L, Mace B, et al. Multi-physics coupling in thermoacoustic devices: A review[J]. Renewable & Sustainable Energy Reviews, 2021, 146.

[5] Cheng C H, Yang H S, Chen H X. Development of a beta-type Stirling heat pump with rhombic drive mechanism by a modified non-ideal adiabatic model[J]. International Journal of Energy Research, 2020, 44(7): 5197-5208.

[6] Wang R Y, Hu J Y, Jia Z L, et al. Study on the temperature adaptability of free-piston Stirling heat pump[J]. Energy Conversion and Management, 2021, 249.

[7] Sun Y L, Hu J Y, Zhang L M, et al. Study on Thermal Technology of Variable Heating Supply Temperature Based on the Duplex Free-Piston Stirling[J]. Journal of Engineering Thermophysics, 2020, 41(7): 1612-1616.

[8] Xu J Y, Hu J Y, Zhang L M, et al. A looped three-stage cascade traveling-wave thermoacoustically-driven cryocooler[J]. Energy, 2016, 112: 804-809.

[9] Xu J Y, Hu J Y, Luo E C, et al. A cascade-looped thermoacoustic driven cryocooler with different-diameter resonance tubes. Part I: Theoretical analysis of thermodynamic performance and characteristics[J]. Energy, 2019, 181: 943-953.

[10] Wang H Z, Zhang L M, Yu G Y, et al. A looped heat-driven thermoacoustic refrigeration system with direct-coupling configuration for room temperature cooling[J]. Science Bulletin, 2019.

[11] Wang K, Herrando M, Pantaleo A M, et al. Technoeconomic assessments of hybrid photovoltaic-thermal vs. conventional solar-energy systems: Case studies in heat and power provision to sports centres[J]. Applied Energy, 2019, 254.

[12] Beijing Municipal Government. 129947. Beijing residential boiler heating management regulations[S]. 1994.

[13] Data of piped natural gas[EB/OL]. [2022-4-25]. https://www.shpgx.com/html/gdtrqsj.html.

[14] National Energy Administration. SY/T 5922-2012. The operation regulation of gas pipeline[S]. 2012.

[15] Herrando M, Markides C N, Hellgardt K. A UK-based assessment of hybrid PV and solar-thermal systems for domestic heating and power: System performance[J]. Applied Energy, 2014, 122: 288-309.

[16] Van Kenhove E, De Vlieger P, Laverge J, et al. Towards energy efficient and healthy buildings: trade-off between Legionella pneumophila infection risk and energy efficiency of domestic hot water systems[J], 2016.
[17] BSI. BS EN 14511-4. Air conditioners, liquid chilling packages and heat pumps for space heating and cooling and process chillers, with electrically driven compressors[S]. 2018.
[18] Lu Y C, Yang D, Tang H L, et al. Trends in urban housing demand[J]. Macroeconomic Management, 2021(11): 34-38.
[19] National Cencus Statistics of 2020[EB/OL]. [2022-4-25]. https://data.stats.gov.cn/easyquery.htm?cn=C01.
[20] Beijing Municipal Institute of City Planning. GB/T 51074-2015. Code for urban heating supply planning[S]. 2015.